ITERATIVE LEARNING CONTROL FOR QUASI-STATIC MEMS MIRROR WITH SWITCHING OPERATION

Matthias Macho[1], Han Woong Yoo[1], Richard Schroedter[2], and Georg Schitter[1]
[1]Automation and Control Institute, TU Wien, AUSTRIA and
[2]Fundamentals of Electrical Engineering, TU Dresden, GERMANY

ABSTRACT

This paper reports an iterative learning control (ILC) to compensate for the errors by the switching operation and the modeling inaccuracies for a quasi-static (QS) MEMS mirror. The modeling errors and uncertainties in dynamics with the switching operation between electrodes result in undesirable oscillations. A wideband frequency-domain ILC is proposed for a QS MEMS mirror with a flatness-based feedforward control. The improvement of the residual oscillations is demonstrated by reduced root mean square (RMS) errors for a 2 Hz and a 2-degree-amplitude sawtooth reference with a factor 69.9.

KEYWORDS

Iterative learning control, quasi static MEMS mirror, electrostatic actuation, switching operation

INTRODUCTION

Electrostatically actuated quasi static micro-electro-mechanical systems (QS MEMS) mirrors enable high quality arbitrary beam positioning with low power consumption via precisely aligned comb drive actuation, typically manufactured by CMOS processes [1]. QS MEMS mirrors require a special design of actuation such as staggered vertical comb (SVC) drives [2], providing beam positioning a wide control bandwidth or tracking a linear scan motion that open vast applications [1,3]. Due to the innate high Q factor, however, control of the QS MEMS mirror is essential to keep the desirable scanning trajectory without overshoot or oscillations. A switching operation for bi-directional scanning can also cause this oscillations.

Various types of controls are applied for QS MEMS mirrors to improve the precision scanning [4-6]. A flatness-based control is designed for QS MEMS mirror with staggered vertical comb (SVC) drives and successfully demonstrates significant reduction of root mean square (RMS) errors down to a few millidegrees [1]. Learning controls such as repetitive control (RC) and iterative learning control (ILC), which improve the control by learning from errors of repeating tasks in the previous trial, are investigated for target scan trajectories to reduce the control errors further with feedback controls [5, 6], while the reductions by the learning controls are mainly noticable in low frequency distortions. For a galvanometer scanner, an ILC strategy with an accurate model demonstrates wideband error compensation beyond two resonances [7]. For QS MEMS mirrors, the compensation solely using ILC for dynamic errors mainly due to switching operations and model inaccuracy has not been studied so far.

PROBLEM DESCIPTION

Model of Quasi-static MEMS Mirror

Figure 1a illustrates the actuation principle of the QS

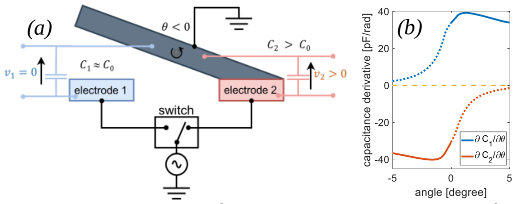

Figure 1: (a) Concept of the electrostatic comb drives for a QS MEM mirror. A voltage is applied between the stator electrode (red and blue rectangles) and the rotor electrode (dark gray), electrostatic torque rotates the mirror toward the turn-on side. The springs on the rotor apply a counter torque. (b) Angular derivative of capacitance for two comb drives along the deflection angle. The sign of $\partial C_1(\theta)/\partial\theta$ and $\partial C_2(\theta)/\partial\theta$ represents the torque direction. Dotted lines represent unused region by the switching operation.

MEMS mirror with two stator electrodes and a rotor electrode [1]. The used QS MEMS mirror is designed by the staggered vertical comb drive technique, allowing the vertical displacement between stator and rotor parts [2]. The deflection θ of the QS MEMS mirror is described by

$$I\ddot{\theta} + b\dot{\theta} + k_m\theta = \frac{1}{2}\frac{\partial C_1(\theta)}{\partial\theta}v_1^2 + \frac{1}{2}\frac{\partial C_2(\theta)}{\partial\theta}v_2^2, \quad (1)$$

where I denotes the inertial of the mirror and rotor, b denotes the damping coefficient, and k_m denotes the mechanical stiffness of the mirror to the frame. Since the mirror and rotor part are suspended by a torsion bar to the frame under the atmospheric air pressure, the mechanical structure is mainly linear with a high Q factor about 90. C_1 and C_2 are the capacitance of the each comb drives and v_1 and v_2 are corresponding stator voltages while rotor is set to ground. When a voltage is applied at either stator electrodes, the mirror rotates toward to the stator by the electrostatic force. Since the torque is generated only by the pulling force, total control u_{tot} can be defined as a normalized torque by the inertia. The sign of the total control can be simply obtained by switching electrodes, i.e.

$$u_{tot} = \begin{cases} \frac{1}{2I}\frac{\partial C_1(\theta)}{\partial\theta}v_1^2 & u_{tot} > 0, \\ \frac{1}{2I}\frac{\partial C_2(\theta)}{\partial\theta}v_2^2 & u_{tot} \leq 0. \end{cases} \quad (2)$$

The direction of the torque is determined by the sign of angular derivative of capacitances as shown in Figure 1b. The total control is then scaled by the angular derivative at the current angle. Due to angular dependency, however, the dynamics become nonlinear in operation and the small model inaccuracy acts as an impulse switching, exciting the main eigenmode of the mirror and resulting in oscillations.

Post-print version of the article: M. Macho, H. W. Yoo, R. Schroedter, G. Schitter, "Iterative Learning Control for Quasi-Static MEMS Mirror with Switching Operation," *2023 IEEE 36th International Conference on Micro Electro Mechanical Systems (MEMS)*pp 538–542, 2023. DOI: 10.1109/MEMS49605.2023.10052637

Variation of Dynamics by Electrostatic Stiffness

The nonlinear angular dependency of the comb drive capacitance causes well-known electrostatic softening or hardening [8]. Assume that only the electrode 1 is activated, i.e. $v_1 > 0$ and $v_2 = 0$, which causes a constant deflection of the mirror at steady-state. Negative voltages of v_1 and v_2 provide the same torque due to the square function. The local dynamics at the operation angle θ_{op} and the stator voltage v_{op} can be approximated as

$$I\Delta\ddot{\theta} + b\Delta\dot{\theta} + k_m\Delta\theta = k_{el}\Delta\theta + K_{el}v_1, \tag{3}$$

$$k_{el} = \frac{1}{2}\frac{\partial^2 C_1(\theta)}{\partial\theta^2}v_1^2\bigg|_{\theta=\theta_{op},\, v_1=v_{op}}, \tag{4}$$

$$K_{el} = \frac{1}{2}\frac{\partial C_1(\theta)}{\partial\theta}v_1\bigg|_{\theta=\theta_{op},\, v_1=v_{op}}, \tag{5}$$

where Δ denotes small changes of the consecutive parameters. The nonlinear torque is represented in a linear manner by the local electrostatic stiffness k_{el} and the local torque constant K_{el}. This leads to the linearized transfer function at the operation point as [1]

$$G_{\Delta\theta/v_1} = \frac{K_{el}}{Is^2 + bs + k_m - k_{el}}. \tag{6}$$

As the electrostatic stiffness is changed by the electrode voltages with the operational angle, the eigenfrequency, of the local dynamics indeed varies by the operation angle. Figure 2a illustrates measured local frequency responses of the dynamics at -1° and -4°, showing discrepancy of local dynamics by a different operational angle [9]. Figure 2b describes the variation of the eigenfrequency and the electrostatic stiffening parameter along the deflection angle. The trend is similar according to the absolute deflection angle while it is not perfectly symmetric. The eigenfrequency varies according to this electrostatic stiffness by the operation angle, which varies most around 0° due to switching operations and the comb configuration.

Flatness-based Feedforward Control and Switching Function

To generate the inputs for the reference trajectory, flatness-based feedforward control is used [1]. The reference trajectory is generated as a smooth jerk limited trajectory, providing reference trajectory with their first and second order differentiation, i.e. $(\ddot{\theta}_{ref}, \dot{\theta}_{ref}, \theta_{ref})$ [10]. Then the flatness-based feedforward control input u_{ff} is obtained by applying the reference trajectory as

$$u_{ff}(\ddot{\theta}_{ref}, \dot{\theta}_{ref}, \theta_{ref}) = \ddot{\theta}_{ref} + \frac{b}{I}\dot{\theta}_{ref} + \frac{k_m}{I}\theta_{ref}. \tag{7}$$

Substitute (2) with (7) as the feedforward control is the total control, the electrode voltages are defined by the switching function as [1]

$$v_{1,ff} = \begin{cases} \sqrt{2Iu_{ff}\left(\dfrac{\partial C_1(\theta_{ref})}{\partial\theta_{ref}}\right)^{-1}} & u_{ff} > 0, \\ 0 & u_{ff} \le 0, \end{cases} \tag{8}$$

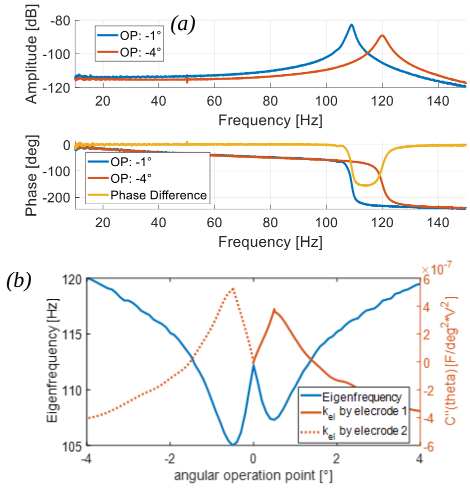

Figure 2: (a) Measured frequency responses of the QS MEMS mirror for different operational angles. (b) Measured eigenfrequency chances over the deflection angle and the estimated electrostatic stiffness k_{el} from the capacitance measurements.

$$v_{2,ff} = \begin{cases} 0 & u_{ff} > 0, \\ \sqrt{2Iu_{ff}\left(\dfrac{\partial C_2(\theta_{ref})}{\partial\theta_{ref}}\right)^{-1}} & u_{ff} \le 0. \end{cases} \tag{9}$$

The trajectory tracking by the feedforward control is highly sensitive to modeling inaccuracies such as the errors in identification of (1), variation of the dynamics of (6), and parasitic motions of the QS MEMS mirror due to imbalanced actuation. With switching, this can lead to large residual errors in scanning trajectories.

ITERATIVE LEARNING CONTROL

Design of Iterative Learning Control

The update equation of frequency-domain ILCs [11], also called IIC [12], is defined by simple multiplications in the Fourier domain via discrete Fourier transform (DFT)

$$\boldsymbol{U}_{j+1}[n] = \boldsymbol{Q}[n]\big(\boldsymbol{U}_j[n] + \boldsymbol{L}[n]\boldsymbol{E}_j[n]\big), \tag{10}$$

$$\boldsymbol{E}_j[n] = \tilde{\boldsymbol{\Theta}}_j[n] - \boldsymbol{\Theta}_{ref}[n], \tag{11}$$

$$\boldsymbol{U}_j[n] = \mathcal{F}\{u_j[k]\} = \sum_{k=0}^{N-1} u_j[k]W_N^{kn}, \tag{12}$$

where $\mathcal{F}$ denotes the Fourier operator, defined with a weights of $W_N = e^{-i2\pi/N}$ and $i = \sqrt{-1}$, and the bold capital notations of $\boldsymbol{U}$, $\tilde{\boldsymbol{\Theta}}$, $\boldsymbol{\Theta}_{ref}$, $\boldsymbol{E}$, $\boldsymbol{L}$, and $\boldsymbol{Q}$ are Fourier coefficients of the ILC input u, measured output $\tilde{\theta}$, reference θ_{ref}, tracking error e, learning filter, and Q filter, respectively. The size N is chosen an integer multiple of the sample number in a scanning period to avoid spectral leakage, i.e. coherent sampling, and n defines the index of harmonic frequency component. For simplicity, $\boldsymbol{Q}$ is chosen as a unity, i.e. $\boldsymbol{Q}(n) = 1, \forall n$, and the learning filter is set to a frequency dependent learning gain ρ with an inversion of estimated QS MEMS mirror dynamics $\widehat{\boldsymbol{G}}$, i.e.

Post-print version of the article: M. Macho, H. W. Yoo, R. Schroedter, G. Schitter, "Iterative Learning Control for Quasi-Static MEMS Mirror with Switching Operation," *2023 IEEE 36th International Conference on Micro Electro Mechanical Systems (MEMS)* pp 538–542, 2023. DOI: 10.1109/MEMS49605.2023.10052637

$\boldsymbol{L}[n] = \rho[n]\widehat{\boldsymbol{G}}^{-1}[n]$. The learning gain is typically below 1 due to convergence, and a smaller learning gain allows more tolerance of modelling errors such as model uncertainty e.g. in (6) and nonlinear switching in (2) at a cost of a slower convergence speed. In this work, the learning gain is chosen as a sharp lowpass filter as $\rho[n] = \rho_0$, for $n \le n_c$, where ρ_0 denotes a constant learning gain and n_c is the index of the cutoff frequency. For $n > n_c$, $\rho[n]$ is set to 0.

ILC with Switching Function

The ILC input u_{j+1} is added to the given feedforward input u_{ff} and together forms the total input, cf. Fig. 3, i.e. $u_{tot,j+1} = u_{ff} + u_{j+1}$. As (8) and (9), the electrode voltages of the ILC are written by

$$v_{1,ILC} = \begin{cases} \sqrt{2Iu_{tot}\left(\frac{\partial C_1(\theta_{ref})}{\partial \theta_{ref}}\right)^{-1}} & u_{tot} > 0, \\ 0 & u_{tot} \le 0, \end{cases} \tag{13}$$

$$v_{2,ILC} = \begin{cases} 0 & u_{tot} > 0, \\ \sqrt{2Iu_{tot}\left(\frac{\partial C_2(\theta_{ref})}{\partial \theta_{ref}}\right)^{-1}} & u_{tot} \le 0. \end{cases} \tag{14}$$

EXPERIMENTAL RESULTS

Experimental Setup and ILC Implementation

Figure 3 describes the experimental setup and the control structure with the QS MEMS mirror. An optical readout by a one dimensional position sensitive device (1D PSD) is used as accurate angle measurements in degree via a calibration procedure by a linear motorized stage [13]. The measured PSD signals are recorded by a dSpace MicroLabBox. The ILC is calculated by Matlab in the PC and generates the electrode voltages by the dSpace MicroLabBox for each electrode via high voltage amplifiers, deflecting the laser beam that shines the PSD.

Figure 3 also illustrates a block diagram of the flatness-based feedforward control and the ILC in the dSpace MicroLabBox. The parameters in (1) for flatness-based feedforward control in (8) and (9) are identified as [1]. The model $\widehat{\boldsymbol{G}}$ is identified based on empirical transfer function estimate (ETFE) via a chirp input signal at the operation angle [14]. The constant learning gain ρ_0 in the learning filter $\boldsymbol{L}$ is set to 0.1, considering model uncertainty and switching nonlinearity of the QS MEMS mirror. The cutoff frequency of $\boldsymbol{L}$ is set to 200 Hz, which is much higher than the eigenfrequency around 114 Hz at 0° to compensate for the oscillations by switching operations. The sampling rate of the dSpace MicroLabBox is set to 50 kHz.

Tracking Results

The flatness-based feedforward control with ILC of (13) and (14) are evaluated and are compared with the feedforward only case of (8) and (9) for sawtooth trajectories with 2° amplitudes for scan rates of 1, 2 and 4 Hz. Figure 4 illustrates the scanning trajectories, input trajectories, and error trajectories of a 2 Hz sawtooth reference trajectory in both cases. The error trajectory of the feedforward control clearly shows undesirable

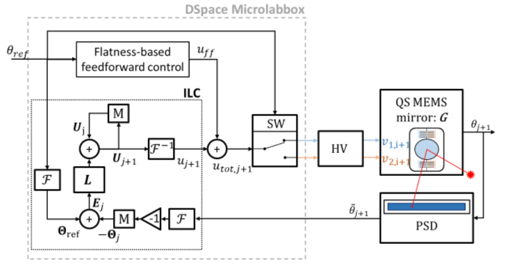

Figure 3: Block diagram of the experimental setup with a frequency-domain ILC. The feedforward input u_{ff} is generated by the reference trajectory θ_{ref}. With the ILC, the total input u_{tot} is applied to the QS MEMS mirror via a switch, steering the laser beam by θ. Then a PSD records the deflection angle of the QS MEMS mirror. With discrete Fourier transform (block $\mathcal{F}$ and $\mathcal{F}^{-1}$), the ILC updates the compensation $\boldsymbol{U_{j+1}}$ from the measured errors of the previous trial $\boldsymbol{E_j}$ from the memories (block M) via learning filter $\boldsymbol{L}$ for improved next trial, $j+1$.

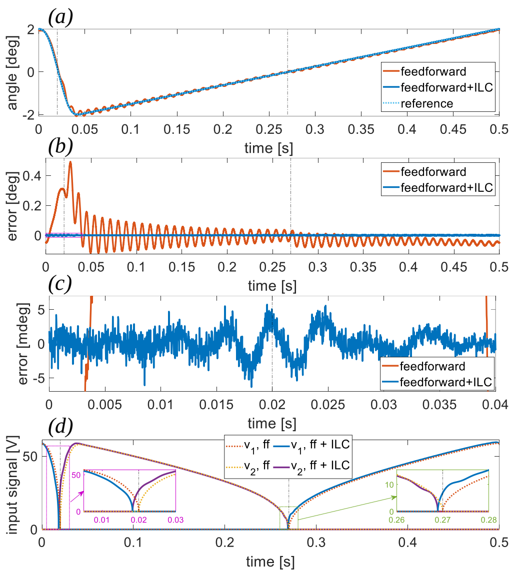

Figure 4: Experimental results of the feedforward control only (red solid lines) and feedforward control with the ILC (blue solid lines) for a 2 Hz sawtooth trajectory with 2° amplitude. (a) Scanning trajectories, (b) residual errors and (c) its zoomed plot near the switching operation (the violet box in (c)). (d) The input trajectories for each electrodes and zoomed plots near the switching operations. Original switching timing is drawn by vertical thin black dashed-dot lines.

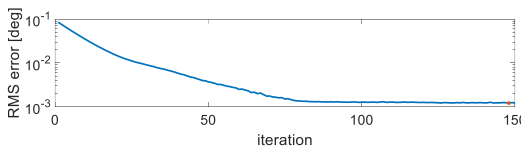

Figure 5: RMS errors along the iteration. The red dot represents the minimum of the RMS error.

Post-print version of the article: M. Macho, H. W. Yoo, R. Schroedter, G. Schitter, "Iterative Learning Control for Quasi-Static MEMS Mirror with Switching Operation," *2023 IEEE 36th International Conference on Micro Electro Mechanical Systems (MEMS)*pp 538–542, 2023. DOI: 10.1109/MEMS49605.2023.10052637

Table 1: RMS errors of a sawtooth reference of 2° amplitude for scan rates of 1, 2, and 4 Hz

Scan rate	RMS Error (mdeg)		Error Ratio
	FF	FF+ILC	(FF/ FF+ILC)
1 Hz	43.9	1.3	35.0
2 Hz	84.8	1.2	69.9
4 Hz	151.2	3.8	39.7

oscillations triggered at the zero angle, where the switching operation between the electrodes happens. The impact of the switching operation is severe at the fast turnaround, generating large oscillations over the linear scanning region of the trajectory by the high Q factor. The switching operation at the slow linear scan region still adds oscillations while the impact is insignificant. The ILC reduces the errors in both phase and the oscillations at the eigenfrequency. The resulting RMS errors are 1.2 milli-degrees with the ILC and 84.8 millidegrees in case of the flatness-based feedforward control only, showing benefits in precise and accurate tracking control. The electrode voltages by the ILC also show the phase correction and oscillations for the compensation.

Figure 5 illustrates the learning transient of the ILC. The main error reduction takes about 80 iterations due to the small learning gain and the minimum is found at 148 iteration. Since ILC can recall the best correction afterwards once the best input is known, the performance can be kept the minimal by the use of the best input. Even if the ILC needs to run again, the number of iteration can be reduced by starting with the best input unless the system changes significantly [11]. Table 1 shows improvements of the sawtooth references for other scan rates. In case of 1 and 4 Hz scan rates the significant RMS error reduction less than 3.8 millidegrees can be achieved. These results demonstrate the feasibility of the proposed ILC for the error compensation of the QS MEMS mirror mainly due to innate nonlinear switching and model inaccuracy, showing potential as a simple and accurate control for QS MEMS mirrors.

CONCLUSION

This paper discusses a frequency-domain iterative learning control to compensate for undesirable oscillations caused by nonlinear switching and model inaccuracy of a QS MEMS mirror. QS MEMS mirrors allow an arbitrary scanning based on CMOS process compatible electrostatic actuation while they require switching to change the torque direction by the zero angle, which can cause unwanted oscillations at the eigenfrequency. A frequency-domain ILC is designed with a low learning gain to cope with this nonlinearity and is implemented with a flatness-based feedforward control to compensate for these undesirable oscillations. The tracking results for sawtooth reference trajectories of 2° amplitude demonstrates the ILC as a highly accurate tracking control, which achieves the RMS error of 1.2 millidegrees from 84.8 millidegrees for the 2 Hz scan rate, leading to an improvement of a factor 69.9 than the flatness-based feedforward control.

ACKNOWLEDGEMENTS

This work has been supported in part by the Austrian Research Promotion Agency (FFG) under the scope of the AUTOScan project (FFG project number 884345). The authors would like to thank David Brunner of Infineon for fruitful discussions.

REFERENCES

[1] R. Schroedter et al., “Flatness-based open-loop and closed-loop control for electrostatic quasi-static microscanners using jerk-limited trajectory design,” *Mechatronics*, vol. 56, pp. 318–331, Dec. 2018,

[2] T. Sandner et al., “Microscanner with vertical out of plane comb drive,” in *16th Int. Conf. on Optical MEMS and Nanophotonics*, pp. 33–34, Aug. 2011.

[3] T. Sandner et al., “Quasistatic microscanner with linearized scanning for an adaptive three-dimensional laser camera,” *J. Micro/Nanolith. MEMS MOEMS*, vol. 13, no. 1, pp. 011114, Feb. 2014,

[4] Y. Zhao, et al., “Fast and precise positioning of electrostatically actuated dual-axis micromirror by multi-loop digital control,” *Sens. Actuator A Phys.*, vol. 132, no. 2, pp. 421–428, 2006.

[5] R. Schroedter et al., “Repetitive nonlinear control for linear scanning micro mirrors,” in *MOEMS and Miniaturized Syst. XVII*, pp. 35, Feb. 2018.

[6] V. Milanović et al., “Iterative learning control (ILC) algorithm for greatly increased bandwidth and linearity of MEMS mirrors in LiDAR and related imaging applications,” in *MOEMS and Miniaturized Syst. XVII*, vol. 10545, pp. 1054513, Feb. 2018.

[7] H. W. Yoo, S. Ito, and G. Schitter, “High speed laser scanning microscopy by iterative learning control of a galvanometer scanner,” *Control Eng. Pract.*, vol. 50, pp. 12–21, May 2016,

[8] A. M. Elshurafa et al., “Nonlinear dynamics of spring softening and hardening in folded-mems comb drive resonators,” *J. Microelectromech. Syst.*, vol. 20, No. 4, pp. 943–958, 2011,

[9] K. Janschek et al., “Adaptive Prefilter Design for Control of Quasistatic Microscanners.” IFAC Proc. Volumes, vol. 46, no. 5, pp. 197–206, 2013,

[10] R. Schroedter et al., "Rasterscan with jerk-limited trajectories for quasi-static/resonant microscanners", *Tagungsband VDI Mechatronik*, pp. 155-160, 2019.

[11] Y. Li and J. Bechhoefer, “Model-free iterative control of repetitive dynamics for high-speed scanning in atomic force microscopy,” *Rev. of Sci. Inst.*, vol. 80, no. 1, pp. 013702, Jan. 2009.

[12] K.-S. Kim and Q. Zou, “A Modeling-Free Inversion-Based Iterative Feedforward Control for Precision Output Tracking of Linear Time-Invariant Systems,” *IEEE/ASME Trans. on Mechatronics*, vol. 18, no. 6, pp. 1767–1777, Dec. 2013.

[13] H. W. Yoo et al., “MEMS Test Bench and its Uncertainty Analysis for Evaluation of MEMS Mirrors,” in *8th IFAC Symp. on Mechatronic Syst.*, vol. 52, no. 15, pp. 49–54, 2019.

[14] L. Ljung, *System Identification: Theory for the User*, 2nd Edition, Prentice-Hall, 1999

CONTACT

*H. W. Yoo, yoo@acin.tuwien.ac.at

Post-print version of the article: M. Macho, H. W. Yoo, R. Schroedter, G. Schitter, “Iterative Learning Control for Quasi-Static MEMS Mirror with Switching Operation,” *2023 IEEE 36th International Conference on Micro Electro Mechanical Systems (MEMS)* pp 538–542, 2023. DOI: 10.1109/MEMS49605.2023.10052637